β-Cell Failure in Diet-Induced Obese Mice Stratified According to Body Weight Gain: Secretory Dysfunction and Altered Islet Lipid Metabolism Without Steatosis or Reduced β-Cell Mass

Marie-Line Peyot,[1] Emilie Pepin,[1] Julien Lamontagne,[1] Martin G. Latour,[1] Bader Zarrouki,[1] Roxane Lussier,[1] Marco Pineda,[1] Thomas L. Jetton,[2] S.R. Murthy Madiraju,[1] Erik Joly,[1] and Marc Prentki[1,3]

OBJECTIVE—C57Bl/6 mice develop obesity and mild hyperglycemia when fed a high-fat diet (HFD). Although diet-induced obesity (DIO) is a widely studied model of type 2 diabetes, little is known about β-cell failure in these mice.

RESEARCH DESIGN AND METHODS—DIO mice were separated in two groups according to body weight gain: low- and high-HFD responders (LDR and HDR). We examined whether mild hyperglycemia in HDR mice is due to reduced β-cell mass or function and studied islet metabolism and signaling.

RESULTS—HDR mice were more obese, hyperinsulinemic, insulin resistant, and hyperglycemic and showed a more altered plasma lipid profile than LDR. LDR mice largely compensated insulin resistance, whereas HDR showed perturbed glucose homeostasis. Neither LDR nor HDR mice showed reduced β-cell mass, altered islet glucose metabolism, and triglyceride deposition. Insulin secretion in response to glucose, KCl, and arginine was impaired in LDR and almost abolished in HDR islets. Palmitate partially restored glucose- and KCl-stimulated secretion. The glucose-induced rise in ATP was reduced in both DIO groups, and the glucose-induced rise in Ca^{2+} was reduced in HDR islets relatively to LDR. Glucose-stimulated lipolysis was decreased in LDR and HDR islets, whereas fat oxidation was increased in HDR islets only. Fatty acid esterification processes were markedly diminished, and free cholesterol accumulated in HDR islets.

CONCLUSIONS—β-Cell failure in HDR mice is not due to reduced β-cell mass and glucose metabolism or steatosis but to a secretory dysfunction that is possibly due to altered ATP/Ca^{2+} and lipid signaling, as well as free cholesterol deposition. *Diabetes* **59:2178–2187, 2010**

While insulin resistance is a common feature in most obese subjects, insulin secretion is increased to compensate for its reduced action and normoglycemia is maintained (1,2). In obese type 2 diabetes subjects, however, β-cell compensation fails due to marked impairment of glucose-stimulated insulin secretion (GSIS), often with reduced β-cell mass (2). The relationship between β-cell function and mass as causative factors in β-cell failure and diabetes progression is debated, with emphasis on the relevance of "functional β-cell mass" rather than total mass (2). Increased adiposity leads to elevated circulating free fatty acids (FFAs) and triglycerides, and in vitro and in vivo studies have indicated a causative role for dyslipidemia in insulin resistance (1,3). Although FFAs are necessary for the amplification of GSIS, their excess supply may also have a role in β-cell failure (4), as prolonged elevation of FFA levels both in vivo and in vitro cause β-cell dysfunction (5,6) and, at least in vitro, apoptosis (7).

At least part of the β-cell compensation to insulin resistance is due to an increase in β-cell mass (4). Either long-term high-fat diet (HFD) (8) or a short-term lipid infusion (9) can result in increased β-cell mass without augmentation of GSIS, indicating that β-cell function and mass are not necessarily linked. Rodent studies have indicated that HFD leads to increased β-cell mass (8), which is also observed in normoglycemic obese individuals (10). Unclear at present is the dynamics between the factors driving compensatory increase in β-cell mass and function and those reducing them through the various stages of type 2 diabetes development, particularly as FFA may do both. Genetic islet susceptibility may be a critical determinant of these dynamics, both in humans and animal models (4,11,12).

Even though studies employing genetically modified models (e.g., Zucker Diabetic Fatty rats, *db/db* mice) have helped in understanding some of these pathological processes (13–16), several of these models are of extreme nature, with rapid development of pronounced type 2 diabetes. These models, therefore, differ from human obesity-linked type 2 diabetes, which usually develops more gradually. In an attempt to gain insight into the basis of β-cell failure in a mild model of diabetes, we recently developed a new model of type 2 diabetes, the 60% pancreatectomized obese hyperlipidemic Zucker Fatty rat (14). In this model, severe β-cell dysfunction was found

without any evidence of a falling β-cell mass or islet steatosis (14). More detailed examination of the pancreatectomized Zucker Fatty rat islets showed marked depletion of insulin stores and altered glycerolipid metabolism (14). The Zucker Fatty rat, as opposed to the Zucker Diabetic Fatty rat, however, does not have genetic predisposition to diabetes, as it maintains normoglycemia despite severe obesity-related insulin resistance (4). The diet-induced obese (DIO) C57BL/6 mouse gradually develops hyperglycemia (17). This suggests that DIO islets are unable to fully compensate for the obesity-related insulin resistance, as occurs in human type 2 diabetes.

In the present study, we investigated β-cell dysfunction in DIO mice stratified into two groups according to the effect of HFD on body weight: the low responders to HFD (LDR) were less obese, developed intermediate severity of insulin resistance, and had only mild impairment in glycemia. The high responders to HFD (HDR) were more obese, insulin resistant, and hyperinsulinemic and were clearly hyperglycemic. Thus, the LDR and HDR groups allowed for analysis and comparison of islet β-cell mass and function in response to different levels of insulin resistance with corresponding very mild perturbation of glucose homeostasis and overt but mild hyperglycemia, respectively. When extended to obese humans, these two groups correspond to the pre-diabetes and early diabetes situations.

RESEARCH DESIGN AND METHODS

Animals and diets. Five-week-old male C57BL/6 mice on a pure genetic background were purchased from Charles River Laboratories (St-Constant, QC, Canada). We verified by RT-PCR analysis that this mouse strain does not harbor a mutation in the nicotinamide nucleotide transhydrogenase gene found in the C57BL/6J strain (18) (data not shown). They were housed 3–4 per cage on a 12-h light/dark cycle at 21°C with free access to water and standard diet (Teklad Global 18% protein rodent diet; Harlan Teklad, Madison, WI, 15% fat by energy). One week after arrival, mice were fed with either the standard or HFD (Bio-Ser Diet #F3282, Frenchtown, NJ, 60% fat by energy) for 8 weeks. Body weight and energy intake were measured weekly. For the energy-intake measurement, the mice were placed in individual cages. Fed blood glucose was determined by a portable glucometer (Accu-check Advantage, Roche, Indianapolis, IN). All procedures were approved by the Institutional Committee for the Protection of Animals at the Centre Hospitalier de l'Université de Montréal.

Plasma parameters. Blood was collected between 8:00 and 10:00 A.M. in fed mice. Plasma insulin and proinsulin were measured by radioimmunoassay (Linco Research, St. Charles, MO) and by ELISA (proinsulin mouse kit, Alpco Diagnostics, Salem, NH), respectively. Plasma nonesterified fatty acids (NEFA) were assessed using the NEFA C kit (Wako Chemical, Osaka, Japan). Plasma triglyceride was determined with the GPO Trinder kit (Sigma Aldrich, Saint Louis, MS), and cholesterol was determined with the Amplex red assay kit (Molecular Probes, Eugene, OR).

Glucose homeostasis, insulin action, and secretion in vivo. Two-hour hyperinsulinemic euglycemic clamp (HIEC) studies were performed in 2-h–fasted, anesthetized normal diet, LDR, and HDR mice after 8 weeks on the experimental diets (19). An intravenous glucose tolerance test (IVGTT) (0.5 g/kg) was conducted in 16-h overnight fasted mice (20). An oral glucose tolerance test (OGTT) (1 g/kg) was also made in 6-h–fasted mice (20). Blood glucose was measured using a portable meter, and plasma insulin was measured using the UltraSensitive mouse Insulin ELISA Kit (Alpco Diagnostics).

β-Cell proliferation and mass. These parameters were measured as described (21).

Islet isolation and culture. Islets were isolated as described (22) and kept in culture at 3 mmol/l glucose for 2 h in RPMI medium supplemented with 10% FBS (complete RPMI) at 37°C, for recovery (23).

Insulin secretion ex vivo. For static incubations, batches of 10 islets each were distributed in 12-well plates and preincubated for 45 min at 37°C in Krebs-Ringer bicarbonate containing 10 mmol/l HEPES (pH 7.4) (KRBH), 0.5% defatted BSA (d-BSA), and 3 mmol/l glucose. They were then incubated for 1 h in KRBH/0.5% d-BSA at 3, 8, and 16 mmol/l glucose or with 35 mmol/l KCl, in the presence or absence of 0.25 mmol/l palmitate. After 1 h, media were kept for insulin measurements by radioimmunoassay. Islet insulin and proinsulin

contents were measured following acid–ethanol (0.2 mmol/l HCl in 75% ethanol) extraction by radioimmunoassay and ELISA, respectively. For perifusion experiments, batches of 120 cultured islets each were placed in perifusion chambers at 37°C and perifused at a flow rate of 1 ml/min for 30 min in KRBH/0.5% d-BSA at 3 mmol/l glucose before stimulation with 16 mmol/l glucose for 60 min and then with 10 mmol/l arginine for 10 min. Islets were then perifused at 3 mmol/l glucose for 30 min.

Intracellular calcium. Ca^{2+} was measured using a modified version of a procedure previously described (24). Dispersed-islet cells from 350–500 freshly isolated islets were plated on 42 mm coverslip and incubated at 37°C overnight in complete RPMI at 11 mmol/l glucose. Cells loaded with Fluo-4 AM calcium indicator were perifused with KRBH/1% d-BSA, 2.5 mmol/l probenicid, 0.2 mmol/l sulfinpyrazone, 0.1 mmol/l IBMX, and 3 or 16 mmol/l glucose or 3 mmol/l glucose + 35 mmol/l KCl. Computational analysis was done using measurements every 3 s. An average of 25 cells per coverslip was analyzed.

Intracellular ATP content. Batches of 50 islets cultured and preincubated as described for insulin secretion experiments were incubated for 15 min in KRBH/0.07% d-BSA at 3 or 16 mmol/l glucose. At the end of the incubation, ATP was extracted from islets and assayed as described (22).

Islet triglyceride, cholesterol, and protein contents. Triglyceride, cholesterol, and protein contents were measured in batches of 100, 40, and 20 freshly isolated islets, respectively (23,25).

Lipid metabolism. For lipolysis, 60 islets per determination were used (23). Fatty acid oxidation and esterification into cholesterol ester were measured in batches of 50 islets (14). NEFA content and fatty acid esterification into triglyceride in 50 islets were determined as described (26).

Glucose metabolism. Islet glucose usage and oxidation were measured as described (22).

Quantitative RT-PCR. See supplemental Research Design and Methods in the online appendix, which is available at http://diabetes.diabetesjournals.org/cgi/content/full/db09-1452/DC1.

Statistical analysis. Data are expressed as means ± SE. Statistical significance was calculated by one-way or two-way ANOVA with Bonferroni, Tukey, or Dunnett post hoc testing as indicated. A P value of <0.05 was considered significant.

RESULTS

Metabolic characteristics of LDR and HDR mice. For mechanistic analyses, pooling mice with markedly different characteristics (for example, little weight gain, no insulin resistance, and normoglycemia with animals with high weight gain, insulin resistance, and hyperglycemia), as has been done in the vast majority of studies so far, can be misleading. We reasoned that this caveat can be dealt with by stratifying mice in two groups (LDR and HDR, as described below) that correspond on one hand to lower weight gain and mild perturbation in glucose homeostasis and on the other hand to higher weight gain and overt but mild hyperglycemia. On the basis of the heterogeneous weight response to diet (∼12 g range for DIO mice housed by group of 3–4 per cage or individually) (Fig. 1A), DIO mice were segregated into two groups after 7.5 weeks on HFD: LDR mice, representing 40% of the DIO mice and weighing 33–38.9 g (lower 6 g range) with an average fed glycemia of 8.6 ± 0.1 mmol/l, and HDR mice, representing 52% of the DIO mice and weighing 39–45 g (higher 6 g range) with an average glycemia of 9.4 ± 0.1 mmol/l (Fig. 1B). DIO outlier mice weighing <33g (∼4% of total DIO mice) and >45g (∼4%) were excluded from this study (Fig. 1A). The control group fed with the standard diet (normal diet) had an average weight of 28.3 ± 0.2 g and a glycemia of 7.5 ± 0.1 mmol/l (Fig. 1B). Difference in body weight in DIO mice was already present after 1 week under HFD and steadily increased during the 8 weeks of the study (Fig. 1C). The considerably larger weight of HDR mice can be accounted, at least in part, to an increased energy intake (106.8 ± 1.4 versus 98.3 ± 1.4 kcal/week in LDR mice, Fig. 1D, inset). Table 1 shows that over 8 weeks HFD-fed LDR and HDR mice, respectively, gained ∼2–3 and 3–4 times more weight compared to normal diet mice. LDR
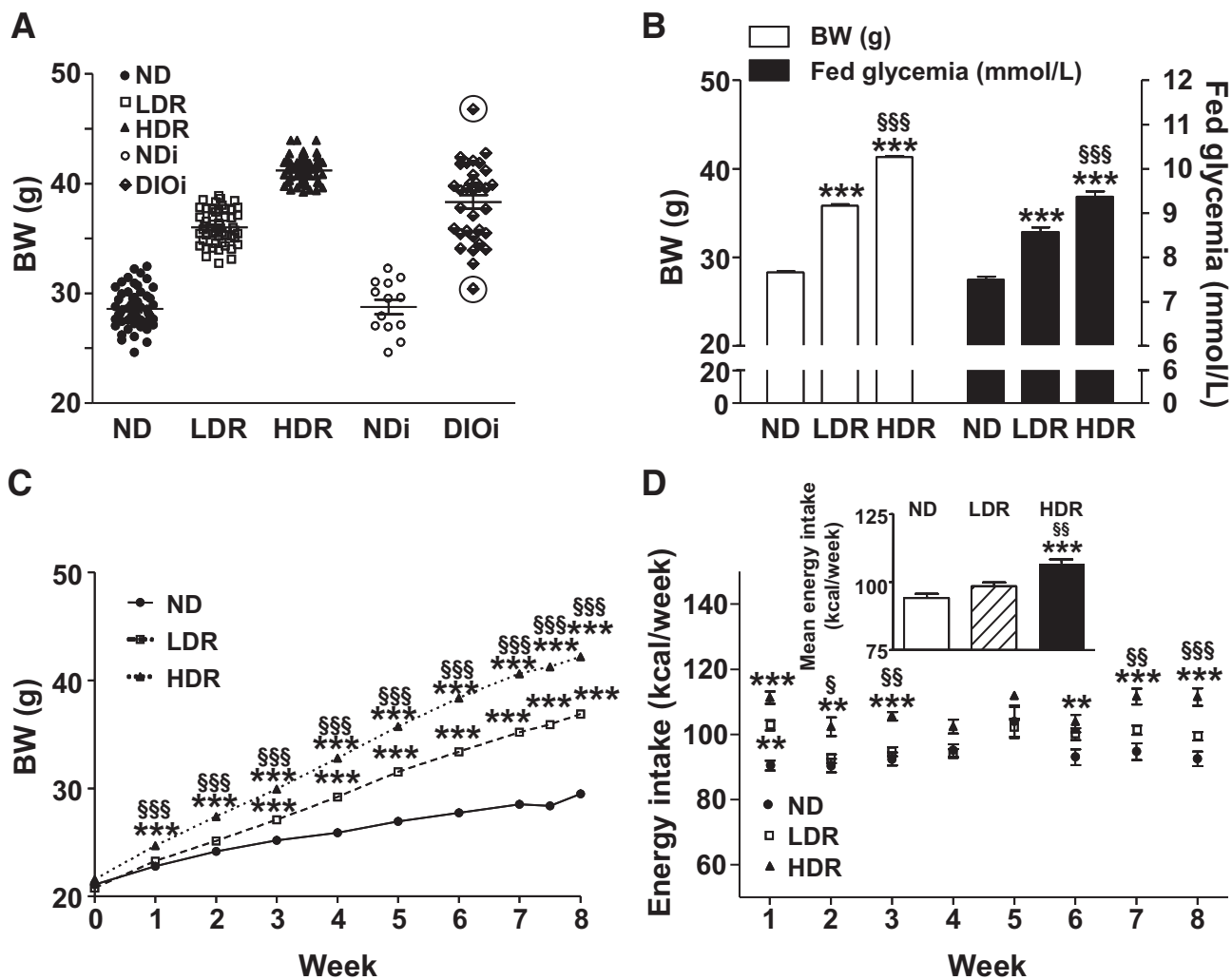
FIG. 1. Body weight (BW), energy intake, and glycemia of C57Bl/6 mice fed normal diet (ND) or HFD for 8 weeks. DIO mice were classified after 7.5 weeks on HFD as LDR and HDR following body weight determinations. *A*: Distribution plots of body weight at 7.5 weeks of ND or HFD mice housed 3–4 per cage (ND, LDR, and HDR) or individually (NDi and DIOi). Encircled symbol corresponds to DIO mice excluded from the study. *B*: Fed glycemia and body weight of ND, LDR, and HDR mice after 7.5 weeks of dietary treatment. (*C*) Weight and (*D*) energy intake curves of ND, LDR, and HDR mice during 8 weeks of ND or HFD. *D, inset*: Mean of energy intake per week per group. *A*: Means ± SE of 52 mice for ND, LDR, and HDR, of 13 and 33 mice for NDi and DIOi, respectively. *B* and *C*: Means ± SE of 136, 117, and 148 mice for the ND, LDR, and HDR groups, respectively. *D*: Means ± SE of 13, 14, and 17 mice for the ND, LDR, and HDR groups, respectively. ND versus LDR or HDR, **$P < 0.01$, ***$P < 0.001$; LDR versus HDR, §$P < 0.05$, §§$P < 0.01$, §§§$P < 0.001$; one-way (*B*) or two-way ANOVA (*C* and *D*), Bonferroni post hoc test.

mice had a very slightly raised glycemia in the fed state (Fig. 1*B*). The 2-h fasting blood glucose of LDR mice was not significantly increased (Fig. 2*A*). In contrast, the HDR group showed a more prominent hyperglycemia than LDR mice. Blood glucose in HDR mice was increased in awake fed mice (9.4 ± 0.1 vs. 7.5 ± 0.1 mmol/l in normal diet mice, Fig. 1*B*)

TABLE 1
Metabolic parameters of C57Bl/6 mice fed with normal diet or HFD for 8 weeks

	Fed			Fasted		
	Normal diet	LDR	HDR	Normal diet	LDR	HDR
Weight gain (g)	8.5 ± 0.2 (62)	15.5 ± 0.2*** (60)	20.4 ± 0.2***,§§§ (72)	5.5 ± 1.0 (5)	16.9 ± 0.6*** (5)	21.0 ± 0.3***,§§ (5)
Insulin (pmol/l)	252 ± 24 (59)	266 ± 20 (58)	658 ± 54***,§§§ (67)	133 ± 87 (5)	338 ± 84 (5)	503 ± 40* (5)
ProIns (pmol/l)	18.5 ± 2.3 (8)	23.7 ± 1.9 (9)	31.8 ± 4.0* (9)	ND	ND	ND
ProIns/Ins (%)	7.8 ± 1.3 (8)	9.4 ± 1.4 (9)	5.5 ± 0.9§ (9)	ND	ND	ND
FFA (mmol/l)	0.60 ± 0.04 (33)	0.55 ± 0.03 (33)	0.58 ± 0.03 (38)	0.77 ± 0.06 (5)	1.12 ± 0.06 (5)	1.58 ± 0.30* (5)
TG (mmol/l)	0.41 ± 0.02 (33)	0.32 ± 0.01*** (34)	0.33 ± 0.01*** (38)	0.36 ± 0.04 (5)	0.40 ± 0.04 (5)	0.39 ± 0.03 (5)
TC (mmol/l)	1.50 ± 0.07 (8)	1.90 ± 0.14 (8)	2.58 ± 0.21***,§ (8)	ND	ND	ND

Data are means ± SE of *n* animals as indicated in parentheses. Plasma triglyceride (TG), FFAs, TC, proinsulin (ProIns), and insulin (Ins) were determined in anesthetized overnight fasted and/or fed male mice on a high-fat diet (LDR and HDR) or normal diet for 8 weeks. Delta body weight represents the weight gain of mice since the introduction of diets (normal diet or HFD) at 6 weeks of age. LDR or HDR versus normal diet: *$P < 0.05$, **$P < 0.01$, ***$P < 0.001$; HDR versus LDR: §$P < 0.05$, §§$P < 0.01$, §§§$P < 0.001$. One-way ANOVA–Bonferroni multiple comparison test. ND, not determined.
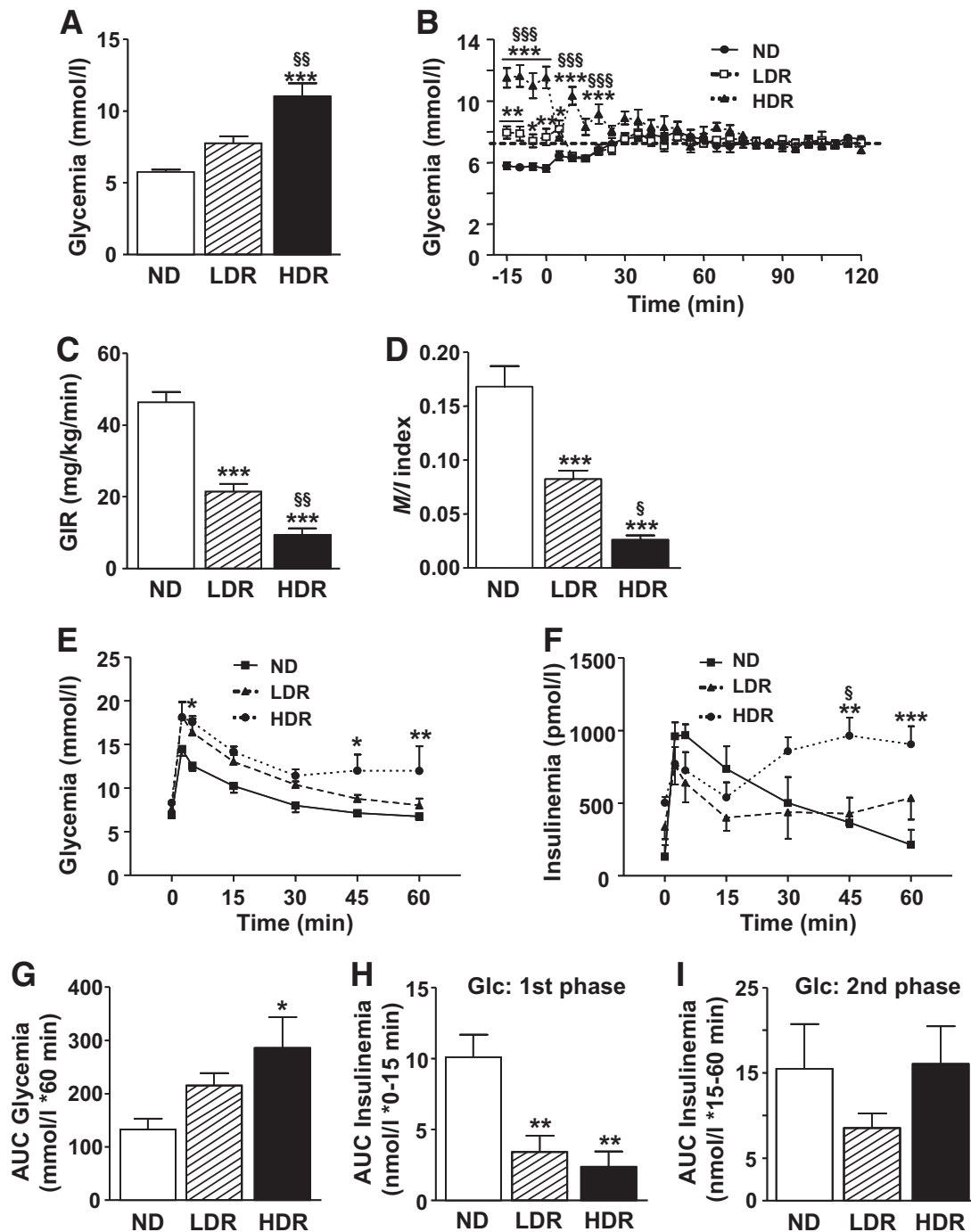
FIG. 2. DIO mice are insulin-resistant, are glucose-intolerant, and have defective first-phase GSIS. *A* and *B*: HIEC in 2-h–fasted anesthetized mice. *A*: Arterial glucose levels at time 0 of the clamp; *B*: glucose levels during the clamp. The dashed line corresponds to the clamped glucose value at ~7.2 mmol/l. (*C*) Glucose infusion rate during the last 30 min of the 2-h HIEC (GIR) and (*D*) insulin sensitivity index (*M/I*) calculated as the glucose infusion rate (*M*) divided by the average insulinemia during the last 30 min of the clamp (*I*). *M/I* index is expressed as $\mu mol \cdot kg^{-1} \cdot min^{-1}$ glucose infused per pmol/l insulin. *E–I*: IVGTT. Plasma glucose (*E*) and insulin (*F*) were measured at times 0, 3, 5, 15, 30, 45, and 60 min in response to a glucose challenge (i.v.; 0.5 g/kg) in 16-h overnight fasted anesthetized mice; (*G*) AUC of the 0–60 min glycemic responses; (*H*) first-phase insulin response to glucose (Glc) is the AUC of the 0–15 min insulinemic response; (*I*) second-phase insulin response to glucose is the AUC of the 15–60 min insulinemic response. Means ± SE of 5–8 animals per group. Normal diet (ND) versus LDR or HDR: *$P < 0.05$, **$P < 0.01$, ***$P < 0.001$; LDR versus HDR: §$P < 0.05$, §§$P < 0.01$, §§§$P < 0.001$; one-way (*A*, *C*, *D*, and *G–I*) or two-way ANOVA (*B*, *E*, and *F*), with Bonferroni post hoc test.

and in 2-h–fasted, anesthetized mice (11.0 ± 0.9 vs. 5.7 ± 0.5 mmol/l in normal diet mice, Fig. 2*A*). Glucose levels in 6-h–fasted HDR mice versus normal diet mice (11.6 ± 0.5 vs. 7.4 ± 0.3 mmol/l) were elevated, and the LDR group showed intermediate values (9.8 ± 0.4 mmol/l) (supplementary Fig. 1*A* and *C*, available in an online appendix). Glycemia in overnight 16-h–fasted HDR mice with anesthesia was slightly

elevated, without reaching statistical significance (8.3 ± 0.3 vs. 7.0 ± 0.4 mmol/l, Fig. 2*E*). Glucose values at time 60 min during an IVGTT (Fig. 2*E*) and time 120 min during an OGTT (supplementary Fig. 1*A* and *D*) remained markedly elevated in HDR, in contrast to the LDR mice. Fasting and fed insulinemia were 3–4-fold higher in the HDR compared to normal diet mice, whereas in LDR mice, fed insulinemia was
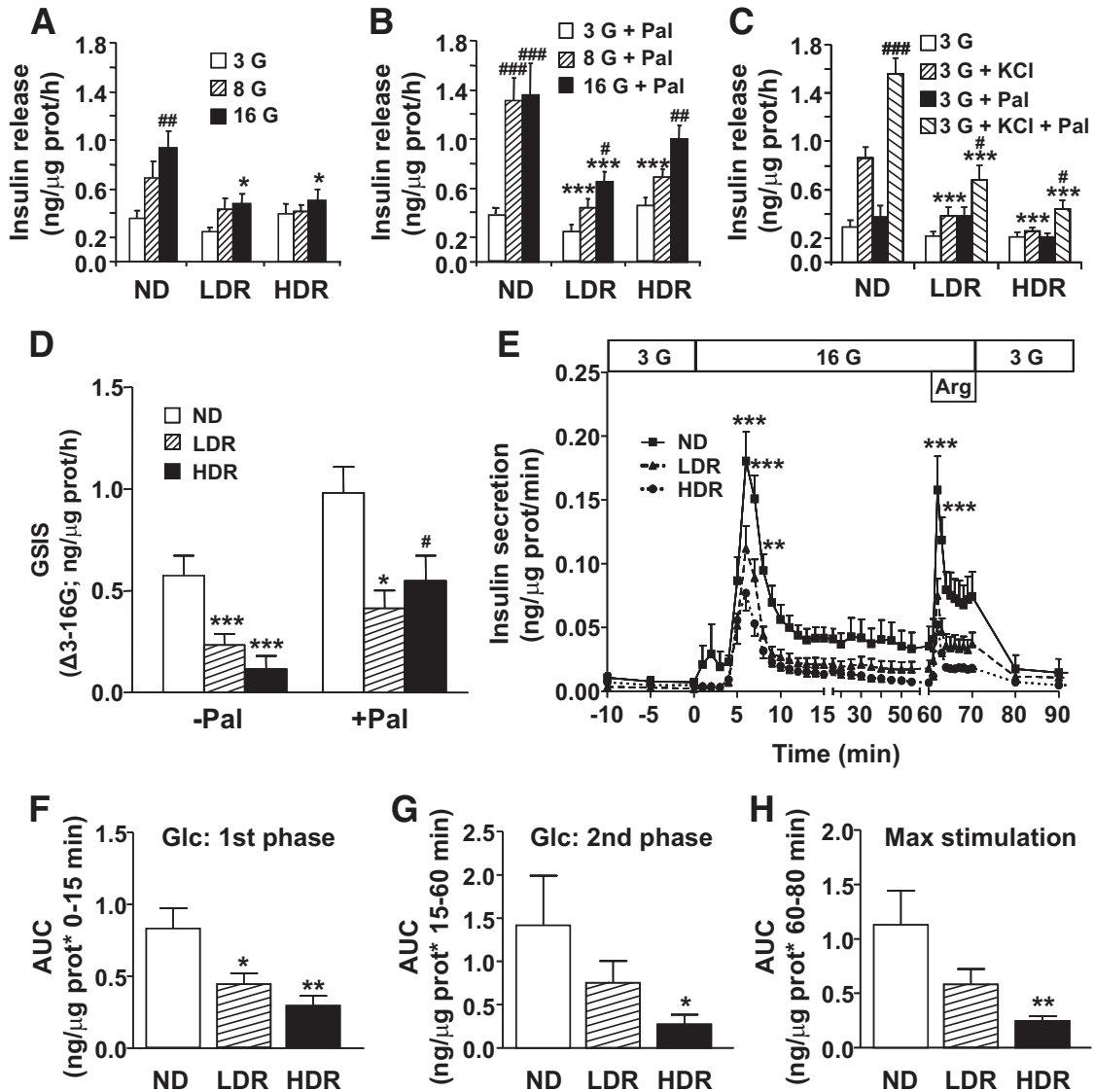
FIG. 3. Isolated islets from DIO mice show defective glucose-, KCl-, and arginine-induced insulin release. Insulin secretion was measured in freshly isolated islets from normal diet (ND), LDR, and HDR mice. Group of 10 islets were incubated 1 h in KRBH at 3, 8, or 16 mmol/l glucose (G; *A* and *D*) ± 0.25 mmol/l palmitate/0.5% d-BSA (Pal; *B* and *D*) or 3 mmol/l glucose ± 35 mmol/l KCl (*C*) ± Pal (*C*). Means ± SE are of 14–16 determinations from islets of 21–22 animals per group in five (*A*, *B*, and *D*) and three (*C*) separate experiments. *E–H*: Insulin secretion by islets perifused at 3 mmol/l glucose (3G) or 16 mmol/l glucose (16G) with or without 10 mmol/l arginine (Arg). AUC for insulin over the first 15 min (*F*) and from 15–60 min (*G*) following glucose concentration increased from 3 to 16 mmol/l. AUC for maximal insulin secretion was determined from 60–80 min after arginine injection (*H*). Means ± SE are of six normal diet, seven LDR, and seven HDR. Insulin release in the media was determined after the 1-h incubation or at the different time points of the perifusion experiment. *$P < 0.05$, **$P < 0.01$, ***$P < 0.001$ normal diet versus LDR or HDR; #$P < 0.05$, ##$P < 0.01$, ###$P < 0.001$ versus 3 mmol/l glucose (*A*) plus palmitate (*B*) or plus KCl (*C*) or versus the value in absence of palmitate (*D*) for the same group (normal diet, LDR, HDR); one-way ANOVA–Bonferroni multiple comparison test.

unchanged and fasting insulinemia was increased by twofold (not statistically significant) (Table 1). Fed proinsulinemia was higher in HDR mice in comparison to normal diet, and the proinsulin-to-insulin ratio was unchanged in LDR and HDR mice versus controls. Of the measured lipid parameters, when compared to normal diet mice, fed plasma cholesterol was significantly increased by 70% in HDR mice, fasting plasma FFAs were twofold higher in HDR mice, and fed plasma triglyceride was 30% decreased in both DIO groups (Table 1).

LDR and HDR mice are insulin-resistant, are glucose-intolerant, and have a decreased first-phase insulin secretion in response to glucose in vivo. A HIEC was made in 2-h–fasted normal diet and DIO mice (Fig. 2*A–D*). Both the glucose infusion rate (Fig. 2*C*) required to maintain glycemia at ~7.2 mmol/l (Fig. 2*B*) and the insulin

sensitivity index (Fig. 2*D*) were decreased by ~50% and ~80% in LDR and HDR mice, respectively, indicating that HDR mice are more insulin resistant than LDR mice. To measure GSIS in vivo, overnight-fasted DIO and normal diet mice were subjected to an IVGTT (Fig. 2*E–I*). Glucose clearance was reduced in HDR mice (Fig. 2*E*), indicating a decreased glucose tolerance as shown by a twofold increase in the area under the curve (AUC) for glycemia (Fig. 2*G*). LDR mice tended to be glucose intolerant but without reaching statistical significance (Fig. 2*E* and *G*). A similar observation was made using the OGTT (supplementary Fig. 1*A* and *B*). Calculation of the AUC for insulinemia during the first 15 min of the IVGTT, subtracting basal values, indicated that first-phase GSIS is reduced by 66 and 76% in the LDR and HDR groups, respectively (Fig. 2*F* and *H*). However, the AUC for the second-phase
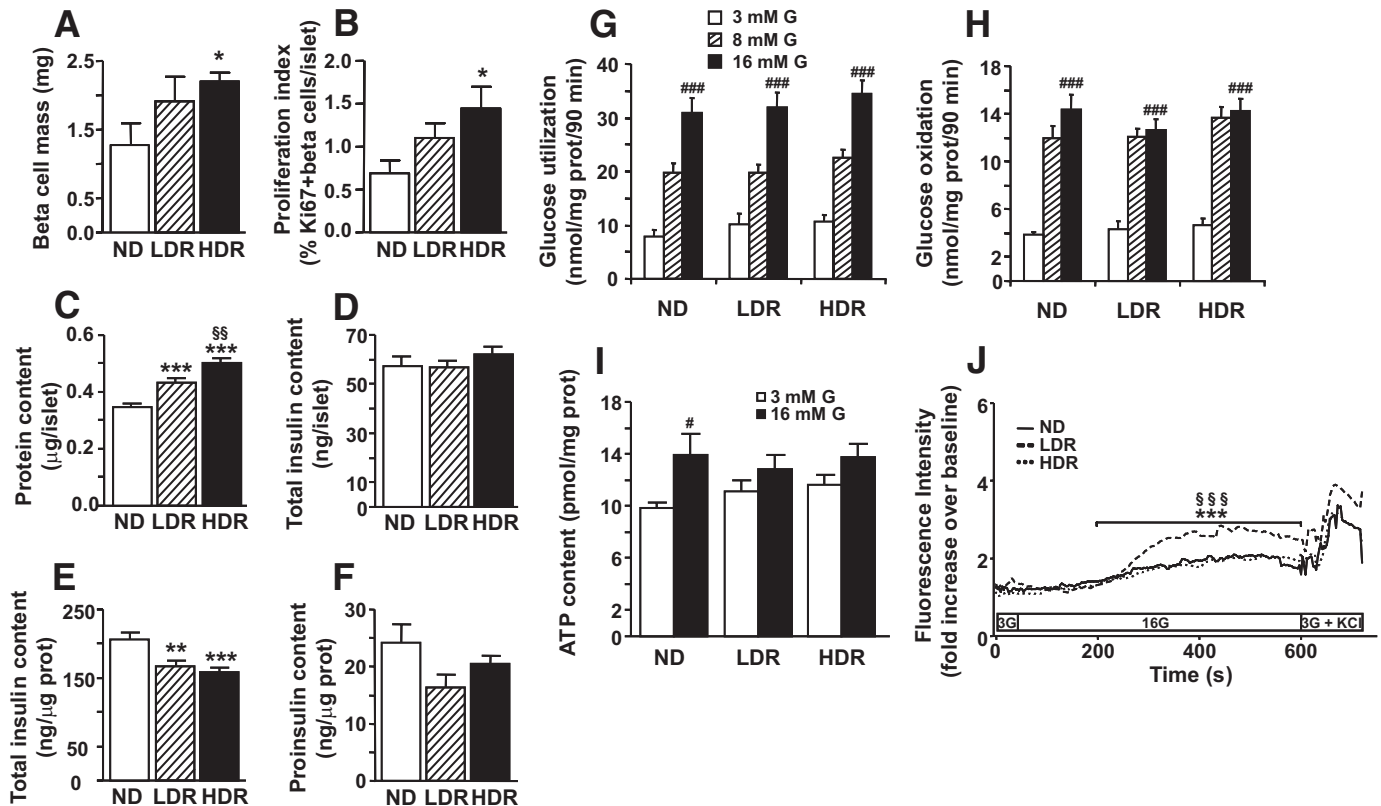
FIG. 4. β-Cell mass and proliferation, islet cell cytosolic free calcium, ATP, proinsulin, insulin and protein contents, and glucose metabolism of DIO mice. (*A*) β-Cell mass and (*B*) proliferation as indicated by the number of Ki-67 positive β-cells/islet. Means ± SE of six animals for normal diet (ND) and LDR and seven for HDR. Normal diet versus LDR or HDR, *P < 0.05. One-way ANOVA with Dunnett post hoc test. (*C*) Protein, (*D* and *E*) insulin expressed per islet (*D*) or per islet protein content (*E*), and (*F*) total islet proinsulin contents. Means ± SE of 83, 35, and 9 animals per group for (*C*), (*D* and *E*), and (*F*), respectively. Normal diet versus LDR or HDR, *P < 0.05, **P < 0.01, and ***P < 0.001; LDR versus HDR, §§P < 0.01. One-way ANOVA with Bonferroni post hoc test. Glucose utilization (*G*) and oxidation (*H*) were measured in islets incubated in KRBH at 3, 8, and 16 mmol/l glucose (*G*) with D-[U-^{14}C]glucose and D-[5-^{3}H]glucose. Means ± SE of 13–15 determinations from islets of 9 normal diet, 8 LDR, and 10 HDR mice in three separate experiments. ###P < 0.001 versus 3 mmol/l glucose for the same group. One-way ANOVA–Bonferroni multiple comparison test. *I*: Total ATP content was determined in islets incubated for 15 min in KRBH at 3 or 16 mmol/l glucose (*G*). Means ± SE of 13–15 determinations from islets of 9 normal diet, 9 LDR, and 9 HDR mice in three separate experiments. #P < 0.05 versus 3 mmol/l glucose for the same group. One-way ANOVA–Bonferroni multiple comparison test. *J*: Cytosolic free calcium was measured by confocal microscopy using Fluo-4 AM dye in dispersed-islet cells of normal diet, LDR, and HDR mice. Cells were perifused for 3 min at 3 mmol/l glucose, then at 16 mmol/l glucose for 10 min, and finally at 3 mmol/l glucose + 35 mmol/l KCl for 2 min. Fluorescence level is expressed in arbitrary units. For clarity purposes, only the mean of six independent experiments from six mice per group is represented. Of note, SE was no more than 15% at all times. One-way ANOVA with repeated measures, Tukey post test. ***P < 0.001 normal diet versus LDR and §§§P < 0.001 LDR versus HDR.

GSIS of both DIO mice was not different from control mice (Fig. 2*F* and *I*).

Impaired insulin secretion in isolated islets from LDR and HDR mice. We next examined GSIS in the presence or absence of exogenous FFA in isolated islets. In normal diet mice, glucose from 3 to 16 mmol/l increased insulin secretion by 2.6-fold (Fig. 3*A*). The glucose effect in both DIO groups was reduced and was almost completely blunted in HDR mice (Fig. 3*A* and *D*). LDR and HDR mice also showed defective KCl-induced insulin secretion (KSIS), with the reduction being more pronounced in the HDR group (Fig. 3*C*). Exogenous palmitate enhanced GSIS in the three groups (Fig. 3*B*) and partially restored GSIS, as evaluated by the difference between high and low glucose values (Fig. 3*D*), as well as KSIS (Fig. 3*C*) in both DIO groups. First-phase GSIS was reduced by 47 and 65% in LDR and HDR perifused islets, respectively (Fig. 3*E* and *F*). HDR mice also showed a fivefold decrease in second-phase GSIS (Fig. 3*G*) and in secretion in response to arginine (Fig. 3*H*).

Lack of decreased pancreatic β-cell mass and islet insulin stores in DIO islets. HDR mice showed a 1.7- and 2-fold increase in β-cell mass (Fig. 4*A*) and prolifera-

tion (Fig. 4*B*), respectively. There was a trend for β-cell mass and proliferation to be increased in the LDR group. Islet protein contents were increased by 24 and 44% in LDR and HDR mice, respectively (Fig. *C*). Total insulin content per islet was similar in all groups (Fig. 4*D*); however, islet content corrected per protein content decreased by 20 and 24% in LDR and HDR islets, respectively (Fig. 4*E*). The islet proinsulin content per protein was similar in all groups (Fig. 4*F*).

Islet glucose metabolism is unchanged in DIO mice. Previous work in type 2 diabetes rodent models has suggested a role for altered glucose metabolism in β-cell dysfunction (27,28). Figure 4 indicates that impaired GSIS in LDR and HDR mice cannot be ascribed to altered glucose metabolism, because glucose usage (Fig. 4*G*) and oxidation (Fig. 4*H*) were unchanged.

Decreased glucose-stimulated ATP content in DIO islets and altered Ca^{2+} signaling in HDR islet cells versus LDR. Normal diet mice showed a 40% increase in intracellular ATP content in response to high glucose, whereas both DIO groups displayed a reduced response (Fig. 4*I*). The rise in Ca^{2+} in response to glucose was markedly larger in LDR versus normal diet islet cells (Fig.
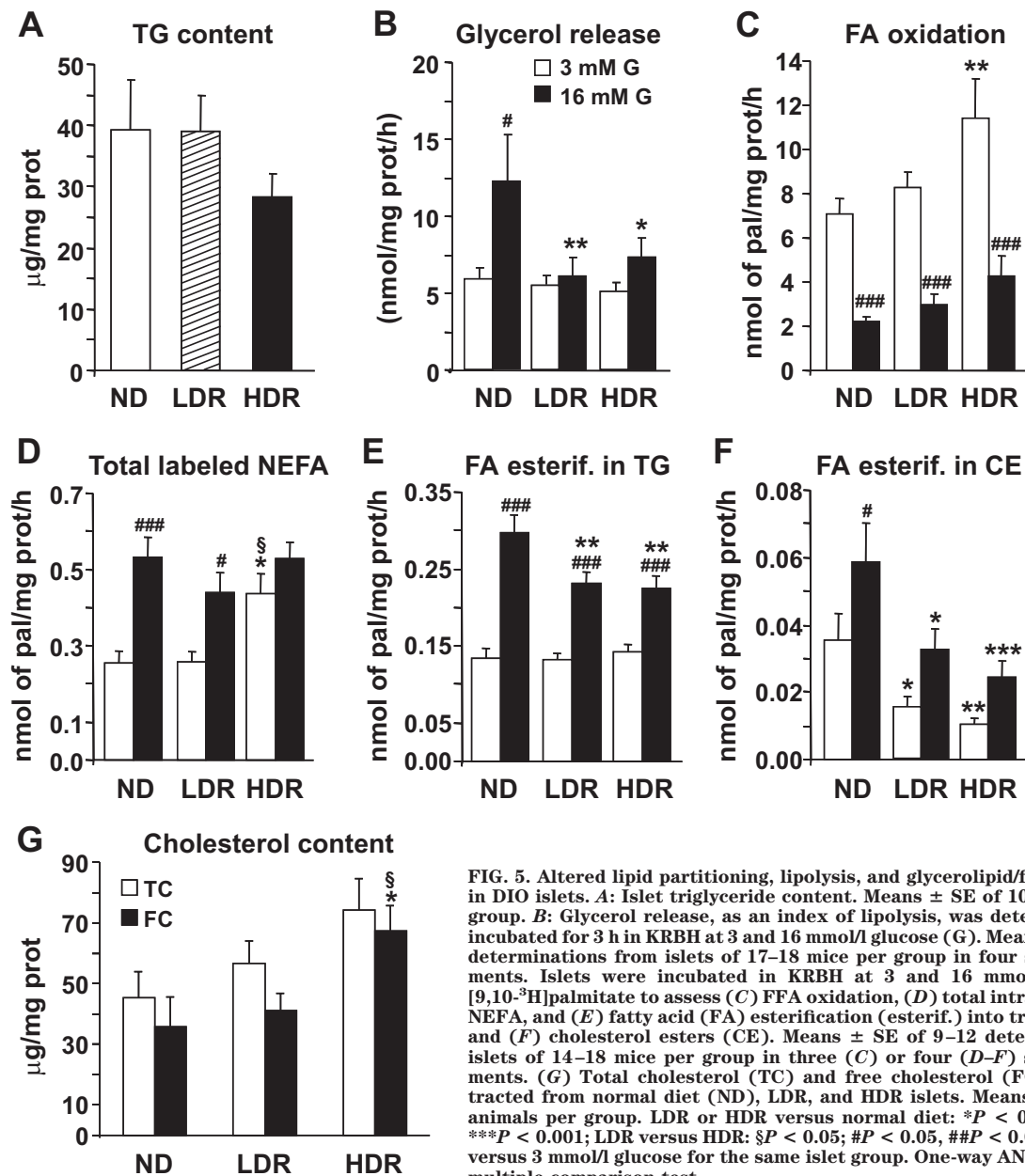
FIG. 5. Altered lipid partitioning, lipolysis, and glycerolipid/fatty acid cycling in DIO islets. *A*: Islet triglyceride content. Means ± SE of 10–12 animals per group. *B*: Glycerol release, as an index of lipolysis, was determined in islets incubated for 3 h in KRBH at 3 and 16 mmol/l glucose (G). Means ± SE of 19–20 determinations from islets of 17–18 mice per group in four separate experiments. Islets were incubated in KRBH at 3 and 16 mmol/l glucose with [9,10-^{3}H]palmitate to assess (*C*) FFA oxidation, (*D*) total intracellular labeled NEFA, and (*E*) fatty acid (FA) esterification (esterif.) into triglycerides (TG) and (*F*) cholesterol esters (CE). Means ± SE of 9–12 determinations from islets of 14–18 mice per group in three (*C*) or four (*D–F*) separate experiments. (*G*) Total cholesterol (TC) and free cholesterol (FC) fractions extracted from normal diet (ND), LDR, and HDR islets. Means ± SE of 10–15 animals per group. LDR or HDR versus normal diet: *P < 0.05, **P < 0.01, ***P < 0.001; LDR versus HDR: §P < 0.05; #P < 0.05, ##P < 0.01, ###P < 0.001 versus 3 mmol/l glucose for the same islet group. One-way ANOVA–Bonferroni multiple comparison test.

4*J*). However, the HDR group did not show such potentiation, which likely reflects a compensation phenomenon. **Altered lipid partitioning, reduced glycerolipid/fatty acid cycling, and free cholesterol deposition in HDR islets.** Islet steatosis was proposed to contribute to β-cell failure (29). However, there was no accumulation of triglyceride in DIO islets (Fig. 5*A*). Work from our group (13,14,22,23) and other groups (30–32) documented a role of β-cell lipolysis and glycerolipid/FFA cycling in insulin secretion. Lipolysis, evaluated by glycerol release, was increased twofold by elevated glucose in normal diet islets (Fig. 5*B*), and this increase was abolished in DIO islets. Fatty acid partitioning (fatty acid oxidation and esterification) was studied in DIO islets since it provides lipid signals for secretion (33). Fatty acid oxidation was similar in both normal diet and LDR islets (Fig. 5*C*). However, fatty acid oxidation was increased by 60% in HDR islets. HDR islets had a 70% higher level of NEFA (an index of long-chain acyl-CoA content) at 3 mmol/l glucose (Fig. 5*D*), consistent with the elevated fatty acid oxidation at

low glucose (Fig. 5*C*). At 16 mmol/l glucose, intracellular NEFA remained not significantly different in all groups (Fig. 5*D*). Glucose-stimulated palmitate esterification into triglyceride was reduced by ~25% in LDR and HDR islets (Fig. 5*E*). An altered lipid esterification process in DIO islets was also evident from the observed reduction in palmitate esterification into cholesterol esters in islets from both DIO groups (Fig. 5*F*). This was associated with a 90 and 60% increase in free cholesterol in HDR versus normal diet and LDR islets, respectively (Fig. 5*G*).

Expression of key transcriptional factors, exocytotic proteins, and enzymes of glucose and lipid metabolism. A panel of mRNA levels was measured to gain insight into the basis of β-cell (de)compensation. Only the mRNA levels of insulin-2, UCP-2 (uncoupling protein-2), SCD-1 (stearoyl-CoA desaturase-1), ACC-2 (acetyl-CoA carboxylase-2), and ATGL (adipose triglyceride lipase) significantly changed in DIO islets (supplementary Figure 2*A–D*, available in an online appendix). Insulin-2 mRNA was increased in both DIO groups, reaching significance only

in HDR islets (supplementary Fig. 2*B*). Increased expression of UCP-2 in the β-cell is thought to play a role in reducing reactive oxygen species production, but the role of UCP-2 in mitochondrial uncoupling or changes in GSIS is debated (34,35). UCP-2 mRNA level was increased by ∼40% in both LDR and HDR islets (supplementary Fig. 2*C*). A 56% increase in ATGL expression, an enzyme involved in triglyceride hydrolysis, was detected in HDR islets (supplementary Fig. 2*C*), which may reflect a compensation phenomenon. In accordance with the increased FFA oxidation in HDR islets (Fig. 5*C*) and the decreased fatty acid esterification in triglyceride in DIO islets (Fig. 5*E*), ACC-2 mRNA was decreased by 45% in HDR islets and SCD-1 mRNA was reduced in DIO islets (supplementary Fig. 2*D*). Thus, SCD-1 is involved in the desaturation of FFA and is important for fatty acid esterification (36), whereas ACC-2 negatively regulates FFA oxidation via the production of malonyl-CoA (37).

DISCUSSION

According to body weight response to HFD, we stratified C57Bl/6 DIO mice in two groups. HDR mice are markedly obese, hyperinsulinemic, insulin resistant, and glucose intolerant and show an altered plasma lipid profile in association with overt but mild hyperglycemia (Table 2). LDR mice have an "intermediate" phenotype and show relatively successful compensation since they are barely glucose intolerant and only very slightly hyperglycemic. Thus, defining these two groups allows the study of the basis of β-cell compensation and failure in two groups of obese mice with the same genetic background and under identical experimental conditions. The HDR group and its comparison with LDR and normal diet mice also allows insight into the causal factors of β-cell failure to sustain the increased demand of insulin in the face of elevated insulin resistance. Importantly, study of HDR and LDR mice may distinguish the alterations in the β-cell that are related to coping with the HFD load and obesity situation from those that may cause β-cell maladaptation to the rising insulin resistance with resulting dysfunction and mild hyperglycemia (the equivalent of pre-diabetes and early diabetes phases in humans).

What is the basis of the β-cell failure to insufficiently compensate for the higher insulin resistance in HDR mice? The results allow the exclusion of several factors (Table 2): decreased β-cell glucose metabolism, islet steatosis, reduced β-cell mass and proliferation, and depletion of insulin stores, because the latter was not significantly decreased per islet and reduced by only 30% if expressed per islet protein in a context where pancreatic β-cell mass increased twofold. However, it cannot be discounted that failure to promote even greater than twofold compensatory increase in β-cell mass, in part, contributed to β-cell failure in the HDR group. Significant β-cell "dedifferentiation" is also unlikely to be involved in β-cell failure of HDR mice because they were markedly hyperinsulinemic, the islet mRNA expression of a large number of genes related to the phenotype of a well differentiated β-cell (PDX-1, MAF-A, Nkx6.1, Glut2, GK, PC, preproinsulin; supplementary Fig. 2*A*) was unchanged, and islet glucose oxidation and usage remained unaltered.

The results point to a role of alterations in the classical ATP/Ca^{2+} signaling and lipid amplification pathways as well as free cholesterol deposition, in the failure of the HDR β-cells to compensate for the marked insulin resistance (Fig. 6). Thus, LDR islets displayed an amplified Ca^{2+} response to glucose that was not apparent in the HDR group, together with reduced rise in ATP content at high glucose, with the latter, however, also being reduced in LDR islets. The reason for the enhanced Ca^{2+} response in the LDR group that should favor compensating insulin secretion remains to be determined. Furthermore, LDR and HDR mice showed altered lipid metabolism and signaling that may explain reduced glucose-, KCl- and arginine-induced insulin secretion. Thus, exogenous palmitate partially restored GSIS and KSIS in islets of both DIO groups. Importantly, the differences that were found between the compensating pre-diabetic LDR and decompensating (here defined as insufficient compensation) HDR groups were enhanced fat oxidation and elevated intracellular NEFA at basal glucose in HDR islets, in association with an increased free cholesterol content, as well as a more pronounced reduction of fatty acid esterification into cholesterol esters and SCD-1 expression (Table 2). Our previous work indicated that both the balance of fat oxidation versus esterification, β-cell lipolysis and GL/FFA cycling play a role in GSIS (13,14). As
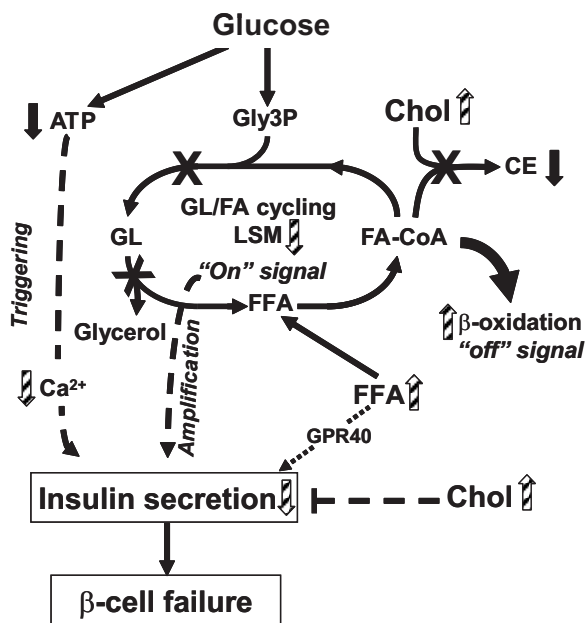
TABLE 2
Summary of the metabolic and islet β-cell parameters obtained in C57Bl/6 male mice fed a high-fat diet for 8 weeks

	LDR	HDR
Metabolic parameters		
Weight gain	↑	↑↑
Insulin resistance	↑	↑↑
Insulinemia	(↑)	↑↑
Proinsulinemia/insulinemia	⇆	⇆
OGTT glucose tolerance	(↓)	↓
ivGTT glucose tolerance	(↓)	↓
ivGTT/1st-phase GSIS	↓	↓↓
ivGTT/2nd-phase GSIS	⇆	⇆
Fasting FFA	(↑)	↑
Fed total cholesterol	(↑)	↑
Fed glycemia	↑	↑↑
2-h–fasted glycemia	(↑)	↑
6-h–fasted glycemia	↑	↑↑
16-h–fasted glycemia	⇆	(↑)
ivGTT, 1 h glucose	⇆	⇆
OGTT, 2 h glucose	(↑)	↑
Islet β-cell parameters		
β-Cell mass	(↑)	↑
β-Cell proliferation	(↑)	↑
Protein content/islet	↑	↑↑
Insulin content/islet	⇆	⇆
Proinsulin content/islet protein	⇆	⇆
Glucose-induced insulin secretion	↓	↓↓
KCl-induced insulin secretion	↓	↓
Glucose usage/oxidation	⇆	⇆
TG content	⇆	⇆
Free cholesterol content	⇆	↑
Glucose-stimulated lipolysis	↓	↓
Glucose effect on NEFA content	(↓)	↓
Glucose effect on FA esterif. in TG	↓	↓
FA esterification in CE	↓	↓↓
FA oxidation	⇆	↑
Glucose-induced ATP	↓	↓
Glucose-induced Ca^{2+}	↑	⇆
KCl-induced Ca^{2+}	⇆	⇆

Horizontal arrow, unchanged versus normal diet–fed animals; arrows in parentheses indicate a clear trend that did not reach statistical significance. FA, fatty acid; TG, triglyceride.

FIG. 6. Model depicting the possible mechanisms of β-cell failure to compensate for insulin resistance in HDR mice. In normal mice, an elevation of glucose leads to an increase in ATP/ADP ratio and intracellular Ca²⁺ and a decrease in fatty acid oxidation that allows long-chain-acyl-CoA (fatty acid-CoA) availability for glycerolipid/fatty acid (GL/FA) cycling, which produces lipid signaling molecules (LSMs), such as diacylglycerol, necessary for insulin secretion. Enhanced GL/FA cycling is an "on" signal for insulin secretion that contributes to the amplification arm of GSIS. Enhanced fat oxidation is an "off" signal for insulin secretion because it removes molecules from the cycle (46). In HDR mice, to adapt to the elevation of circulating FFA and postprandial glucose and to prevent β-cell glucolipotoxicity and steatosis, fatty acid esterification processes and lipolysis are simultaneously decreased in association with enhanced FFA oxidation. The increase in fatty acid oxidation, in parallel to depleting LSM, reduces fatty acid-CoA availability for cholesterol ester (CE) synthesis, contributing with elevated blood cholesterol to free cholesterol accumulation and β-cell dysfunction with reduced secretion. Besides the amplification arm of GSIS, the classical triggering ATP/Ca²⁺ pathway is also affected in HDR versus LDR mice due to reduced glucose-stimulated ATP production and a lack of compensatory increase in the rise in Ca²⁺ promoted by high glucose. GPR40 activation by FFA may contribute to maintain high level of secretion and hyperinsulinemia. However, in the absence of insufficient insulin secretion for the demand due to the marked insulin resistance, HDR mice become hyperglycemic. Black arrows indicate a difference between DIO group (LDR and HDR) and normal diet group. Striped arrows indicate a difference between HDR and LDR groups.

shown in Fig. 6, in HDR mice, impaired glucose-stimulated lipolysis and fatty acid esterification should reduce the production of lipid signaling molecules such as diacylglycerol (33), which has been linked to the activation of C-kinase enzymes (38) and the exocytotic protein Munc13-1 (39), whereas enhanced fat oxidation should simultaneously cause their removal. Increased fatty acid oxidation should also reduce fatty acid-CoA availability for cholesterol ester formation (a protective mechanism against the toxic effects of excess cholesterol) (40) leading to free cholesterol accumulation.

Alteration in β-cell cholesterol metabolism has emerged as a factor contributing to β-cell dysfunction as evidenced in a number of in vitro and in vivo studies (25,41,42). Interestingly, total plasma cholesterol and islet free cholesterol deposition occurred only in the HDR group, illustrating the interest of stratification of DIO groups. Cholesterol is abundant in lipid rafts that are implicated in exocytosis (43), and it can be hypothesized that such modification may contribute to the observed reduction in

insulin secretion in response to all classes of secretagogues. Consistent with this view, Collins et al. (44) observed reduced β-cell exocytosis elicited by short depolarization in DIO mice.

Comparison of in vitro and in vivo insulin secretion of DIO mice indicated that the secretory defect is more prominent in vitro. The nature of the factors allowing compensatory increased (but not sufficient) insulin secretion with hyperinsulinemia in vivo remains to be known and may include FFA as suggested by our in vitro work, enhanced incretin signaling, reduced levels of counterregulatory hormones, and neural pathways (45).

In conclusion, HDR mice fail to fully compensate for the prominent insulin resistance that exacerbates the demand for insulin to maintain euglycemia. HDR islets have a defect in β-cell secretory function in response to glucose and nonfuel stimuli that is possibly caused by 1) a lack of compensatory increase in ATP/Ca²⁺ signaling; 2) free cholesterol accumulation; and 3) impaired lipid signaling due to a metabolic shift with altered lipid partitioning and glycerolipid/FFA cycling. We propose that all three factors contribute to the inappropriate capacity to maintain sufficient secretion in the face of insulin resistance. Additional work is required to define in further details the biochemical basis of β-cell failure in HDR DIO mice.

REFERENCES

1. Kahn SE, Hull RL, Utzschneider KM. Mechanisms linking obesity to insulin resistance and type 2 diabetes. Nature 2006;444:840–846
2. Henquin JC, Cerasi E, Efendic S, Steiner DF, Boitard C. Pancreatic beta-cell mass or beta-cell function? That is the question! Diabetes Obes Metab 2008;10(Suppl. 4):1–4
3. Lowell BB, Shulman GI. Mitochondrial dysfunction and type 2 diabetes. Science 2005;307:384–387
4. Prentki M, Nolan CJ. Islet beta cell failure in type 2 diabetes. J Clin Invest 2006;116:1802–1812

5. Maedler K, Oberholzer J, Bucher P, Spinas GA, Donath MY. Monounsaturated fatty acids prevent the deleterious effects of palmitate and high glucose on human pancreatic beta-cell turnover and function. Diabetes 2003;52:726–733

6. Mason TM, Goh T, Tchipashvili V, Sandhu H, Gupta N, Lewis GF, Giacca A. Prolonged elevation of plasma free fatty acids desensitizes the insulin secretory response to glucose in vivo in rats. Diabetes 1999;48:524–530

7. El-Assaad W, Buteau J, Peyot ML, Nolan C, Roduit R, Hardy S, Joly E, Dbaibo G, Rosenberg L, Prentki M. Saturated fatty acids synergize with elevated glucose to cause pancreatic beta-cell death. Endocrinology 2003;144:4154–4163

8. Hull RL, Kodama K, Utzschneider KM, Carr DB, Prigeon RL, Kahn SE. Dietary-fat-induced obesity in mice results in beta cell hyperplasia but not increased insulin release: evidence for specificity of impaired beta cell adaptation. Diabetologia 2005;48:1350–1358

9. Steil GM, Trivedi N, Jonas JC, Hasenkamp WM, Sharma A, Bonner-Weir S, Weir GC. Adaptation of beta-cell mass to substrate oversupply: enhanced function with normal gene expression. Am J Physiol Endocrinol Metab 2001;280:E788–E796

10. Butler AE, Janson J, Bonner-Weir S, Ritzel R, Rizza RA, Butler PC. Beta-cell deficit and increased beta-cell apoptosis in humans with type 2 diabetes. Diabetes 2003;52:102–110

11. Røder ME, Porte D Jr, Schwartz RS, Kahn SE. Disproportionately elevated proinsulin levels reflect the degree of impaired B cell secretory capacity in patients with noninsulin-dependent diabetes mellitus. J Clin Endocrinol Metab 1998;83:604–608

12. Rahier J, Guiot Y, Goebbels RM, Sempoux C, Henquin JC. Pancreatic beta-cell mass in European subjects with type 2 diabetes. Diabetes Obes Metab 2008;10(Suppl. 4):32–42

13. Nolan CJ, Leahy JL, Delghingaro-Augusto V, Moibi J, Soni K, Peyot ML, Fortier M, Guay C, Lamontagne J, Barbeau A, Przybytkowski E, Joly E, Masiello P, Wang S, Mitchell GA, Prentki M. Beta cell compensation for insulin resistance in Zucker fatty rats: increased lipolysis and fatty acid signalling. Diabetologia 2006;49:2120–2130

14. Delghingaro-Augusto V, Nolan CJ, Gupta D, Jetton TL, Latour MG, Peshavaria M, Madiraju SR, Joly E, Peyot ML, Prentki M, Leahy J. Islet beta cell failure in the 60% pancreatectomised obese hyperlipidaemic Zucker fatty rat: severe dysfunction with altered glycerolipid metabolism without steatosis or a falling beta cell mass. Diabetologia 2009;52:1122–1132

15. Zhou YP, Cockburn BN, Pugh W, Polonsky KS. Basal insulin hypersecretion in insulin-resistant Zucker diabetic and Zucker fatty rats: role of enhanced fuel metabolism. Metabolism 1999;48:857–864

16. Zhou YP, Berggren PO, Grill V. A fatty acid-induced decrease in pyruvate dehydrogenase activity is an important determinant of beta-cell dysfunction in the obese diabetic db/db mouse. Diabetes 1996;45:580–586

17. Surwit RS, Kuhn CM, Cochrane C, McCubbin JA, Feinglos MN. Diet-induced type II diabetes in C57BL/6J mice. Diabetes 1988;37:1163–1167

18. Wong N, Blair AR, Morahan G, Andrikopoulos S. The deletion variant of nicotinamide nucleotide transhydrogenase (Nnt) does not affect insulin secretion or glucose tolerance. Endocrinology 2010;151:96–102

19. Alquier T, Peyot ML, Latour MG, Kebede M, Sorensen CM, Gesta S, Ronald Kahn C, Smith RD, Jetton TL, Metz TO, Prentki M, Poitout V. Deletion of GPR40 impairs glucose-induced insulin secretion in vivo in mice without affecting intracellular fuel metabolism in islets. Diabetes 2009;58:2607–2615

20. Latour MG, Alquier T, Oseid E, Tremblay C, Jetton TL, Luo J, Lin DC, Poitout V. GPR40 is necessary but not sufficient for fatty acid stimulation of insulin secretion in vivo. Diabetes 2007;56:1087–1094

21. Jetton TL, Lausier J, LaRock K, Trotman WE, Larmie B, Habibovic A, Peshavaria M, Leahy JL. Mechanisms of compensatory beta-cell growth in insulin-resistant rats: roles of Akt kinase. Diabetes 2005;54:2294–2304

22. Peyot ML, Guay C, Latour MG, Lamontagne J, Lussier R, Pineda M, Ruderman NB, Haemmerle G, Zechner R, Joly E, Madiraju SR, Poitout V, Prentki M. Adipose triglyceride lipase is implicated in fuel- and non-fuel-stimulated insulin secretion. J Biol Chem 2009;284:16848–16859

23. Peyot ML, Nolan CJ, Soni K, Joly E, Lussier R, Corkey BE, Wang SP, Mitchell GA, Prentki M. Hormone-sensitive lipase has a role in lipid signaling for insulin secretion but is nonessential for the incretin action of glucagon-like peptide 1. Diabetes 2004;53:1733–1742

24. Pepin E, Guay C, Delghingaro-Augusto V, Joly E, Madiraju SR, Prentki M. Short-chain 3-hydroxyacyl-CoA dehydrogenase is a negative regulator of insulin secretion in response to fuel and non-fuel stimuli in INS832/13 β-cells. J Diabetes. 2010 (Available from http://www3.interscience.wiley.com/journal/123371665/abstract?CRETRY=1&SRETRY=0; Accessed Apr 23, 2010)

25. Hao M, Head WS, Gunawardana SC, Hasty AH, Piston DW. Direct effect of cholesterol on insulin secretion: a novel mechanism for pancreatic beta-cell dysfunction. Diabetes 2007;56:2328–2338

26. Peyot ML, Gray JP, Lamontagne J, Smith PJ, Holz GG, Madiraju SR, Prentki M, Heart E. Glucagon-like peptide-1 induced signaling and insulin secretion do not drive fuel and energy metabolism in primary rodent pancreatic beta-cells. PLoS One 2009;4:e6221

27. Ohneda M, Johnson JH, Lee YH, Nagasawa Y, Unger RH. Post-GLUT-2 defects in beta-cells of non-insulin-dependent diabetic obese rats. Am J Physiol 1994;267:E968–E974

28. Fex M, Nitert MD, Wierup N, Sundler F, Ling C, Mulder H. Enhanced mitochondrial metabolism may account for the adaptation to insulin resistance in islets from C57BL/6J mice fed a high-fat diet. Diabetologia 2007;50:74–83

29. Lee Y, Hirose H, Ohneda M, Johnson JH, McGarry JD, Unger RH. Beta-cell lipotoxicity in the pathogenesis of non-insulin-dependent diabetes mellitus of obese rats: impairment in adipocyte-beta-cell relationships. Proc Natl Acad Sci U S A 1994;91:10878–10882

30. Fex M, Haemmerle G, Wierup N, Dekker-Nitert M, Rehn M, Ristow M, Zechner R, Sundler F, Holm C, Eliasson L, Mulder H. A beta cell-specific knockout of hormone-sensitive lipase in mice results in hyperglycaemia and disruption of exocytosis. Diabetologia 2009;52:271–280

31. Mulder H, Yang S, Winzell MS, Holm C, Ahrén B. Inhibition of lipase activity and lipolysis in rat islets reduces insulin secretion. Diabetes 2004;53:122–128

32. Cantley J, Burchfield JG, Pearson GL, Schmitz-Peiffer C, Leitges M, Biden TJ. Deletion of PKCepsilon selectively enhances the amplifying pathways of glucose-stimulated insulin secretion via increased lipolysis in mouse beta-cells. Diabetes 2009;58:1826–1834

33. Nolan CJ, Madiraju MS, Delghingaro-Augusto V, Peyot ML, Prentki M. Fatty acid signaling in the beta-cell and insulin secretion. Diabetes 2006;55(Suppl. 2):S16–S23

34. Produit-Zengaffinen N, Davis-Lameloise N, Perreten H, Bécard D, Gjinovci A, Keller PA, Wollheim CB, Herrera P, Muzzin P, Assimacopoulos-Jeannet F. Increasing uncoupling protein-2 in pancreatic beta cells does not alter glucose-induced insulin secretion but decreases production of reactive oxygen species. Diabetologia 2007;50:84–93

35. Chan CB, De Leo D, Joseph JW, McQuaid TS, Ha XF, Xu F, Tsushima RG, Pennefather PS, Salapatek AM, Wheeler MB. Increased uncoupling protein-2 levels in beta-cells are associated with impaired glucose-stimulated insulin secretion: mechanism of action. Diabetes 2001;50:1302–1310

36. Prentki M, Madiraju SR. Glycerolipid metabolism and signaling in health and disease. Endocr Rev 2008;29:647–676

37. Abu-Elheiga L, Matzuk MM, Abo-Hashema KA, Wakil SJ. Continuous fatty acid oxidation and reduced fat storage in mice lacking acetyl-CoA carboxylase 2. Science 2001;291:2613–2616

38. Biden TJ, Schmitz-Peiffer C, Burchfield JG, Gurisik E, Cantley J, Mitchell CJ, Carpenter L. The diverse roles of protein kinase C in pancreatic beta-cell function. Biochem Soc Trans 2008;36:916–919

39. Kwan EP, Xie L, Sheu L, Nolan CJ, Prentki M, Betz A, Brose N, Gaisano HY. Munc13-1 deficiency reduces insulin secretion and causes abnormal glucose tolerance. Diabetes 2006;55:1421–1429

40. Busch AK, Gurisik E, Cordery DV, Sudlow M, Denyer GS, Laybutt DR, Hughes WE, Biden TJ. Increased fatty acid desaturation and enhanced expression of stearoyl coenzyme A desaturase protects pancreatic beta-cells from lipoapoptosis. Diabetes 2005;54:2917–2924

41. Brunham LR, Kruit JK, Pape TD, Timmins JM, Reuwer AQ, Vasanji Z, Marsh BJ, Rodrigues B, Johnson JD, Parks JS, Verchere CB, Hayden MR. Beta-cell ABCA1 influences insulin secretion, glucose homeostasis and response to thiazolidinedione treatment. Nat Med 2007;13:340–347

42. Hao M, Bogan JS. Cholesterol regulates glucose-stimulated insulin secretion through phosphatidylinositol 4,5-bisphosphate. J Biol Chem 2009;284:29489–29498

43. Xia F, Gao X, Kwan E, Lam PP, Chan L, Sy K, Sheu L, Wheeler MB, Gaisano HY, Tsushima RG. Disruption of pancreatic beta-cell lipid rafts modifies Kv2.1 channel gating and insulin exocytosis. J Biol Chem 2004;279:24685–24691

44. Collins SC, Hoppa MB, Walker JN, Amisten S, Abdulkhader F, Bengtsson M, Fearnside J, Ramracheya R, Toye AA, Zhang Q, Clark A, Gauguier D, Rorsman P. Progression of diet-induced diabetes in C57Bl6J mice involves functional dissociation of Ca2+ channels from secretory vesicles. Diabetes 2010;59:1192–1201

45. Winzell MS, Ahrén B. G-protein-coupled receptors and islet function-implications for treatment of type 2 diabetes. Pharmacol Ther 2007;116:437–448

46. Nolan CJ, Prentki M. The islet beta-cell: fuel responsive and vulnerable. Trends Endocrinol Metab 2008;19:285–291